Optimization of Nusselt Number of Al_2O_3/Water Nanofluid Using Response Surface Methodology

***Motahari, Kazem**+; *Barati, Sara**+**

Department of Chemical Engineering, Faculty of Engineering, Arak University, P.O. Box 38156-8-8349 Arak, I.R. IRAN

ABSTRACT: *This study has primarily aimed at the examination of the effect of flow rate, solid volume fraction and their interactions on the Nusselt number of Al_2O_3/water nanofluids. To investigate the main and interaction effects on the response, Response Surface Methodology (RSM) has been used based on the miscellaneous design. By using the analysis of variance (ANOVA) the significance of the model is tested. The responses to the Nusselt number of nanofluids are also estimated using second-order polynomial equations. The results show that the Nusselt number increases with a higher amount of flow rate and solid volume fraction. According to the analysis of variance, the Reynolds number (A), first and second order of effects of volume fraction (B, B^2), the interaction of Reynolds number and volume fraction (AB) are the most effective factors on the Nusselt number. Finally, the optimum condition of the process is predicted based on the RSM method. Having considered the optimum condition, the Nusselt numbers are compared with experimental data. The results show that there is a good agreement between the results of the proposed model and experimental data. Therefore, according to the results, the Nusselt number is precisely predictable in the model proposed by the Design Expert software.*

KEYWORDS *Nanofluid; Response surface methodology; Heat transfer; Experimental; Analysis of variance.*

INTRODUCTION

For many years, various techniques have been used to improve the heat transfer rate, but the best technique is the one that reduces the size and cost of heat exchangers. Generally, these techniques can be classified into two distinct groups: 1) passive techniques, and 2) active techniques [1-3] passive techniques increase the heat transfer rate by improving the fluid properties, changing flow geometry and boundary conditions [4]. Many researchers have investigated this technique on roughened tubes such as finned tubes, helical tubes, fluted tubes and elliptical axis tubes [5-8]. One of the methods of improving fluid properties is the addition of solid nanoparticles to the fluid. These fluids are called nanofluids. Nanofluids increase the heat transfer rate by changing the properties of the base fluid [9]. Many researchers [10-12] experimentally and numerically have studied the effect of adding nanoparticle to various base fluids on heat transfer. The results showed that in both laminar and turbulent, increasing nanofluid concentration improves heat transfer. Most of the works mentioned

* *To whom correspondence should be addressed.*
\+ *E-mail: dr.motahari@yahoo.com ; sara.barati85@yahoo.com*
1021-9986/2019/3/309-317 9/$/5.09

Table 1: A summary of some experimental and numerical studies.

authors	Base fluid	Nano particle	flows' patterns	method
Wen and et al [13]	water	Al_2O_3	laminar	experimental
S. Zeinali Heris and et al [14]	water	CuO and Al_2O_3	laminar	experimental
Bianco and et al [15]	water	Al_2O_3	turbulent	numerical
Behzadmehr and et al [16]	water	Cu	turbulent	numerical
Hemmat Esfe and et al [17]	water	MgO	turbulent	experimental
Hojjat and et al [18]	carboxymethyl cellulose	γ-Al_2O_3, CuO, and TiO_2	turbulent	experimental
Suresh and et al [19]	water	Al_2O_3–Cu	laminar	experimental
Duangthongsuk [20]	water	TiO_2	turbulent	experimental

above tried to investigate the influence of the velocity and the nano-particles concentration on the heat transfer of nanofluids. Table 1 summarized some experimental and numerical studies for the heat transfer enhancement of nanofluids in both laminar and turbulent regimes. Base on the author's knowledge, there are little studies focused on the optimum conditions for effective parameters in heat transfer.

Response Surface Methodology (RSM) is a collection of mathematical and statistical techniques for building an empirical model. An experiment includes a series of tests or runs. In each run, one of the input variables changes, and its responses appear within the output variables subsequently. According to the runs, the desirable relationship between effective parameters and responses can be detected. The objective of the design of the experiment is to optimize output which is influenced by several independent input variables. The purpose of this study is to utilize the design of experiment for prediction of the Nusselt number of Al_2O_3/water nanofluid at different solid volume fraction and flow rate (Reynolds number) and their interactions. In addition, after predicting an optimal condition using RSM method, an experiment has been done to evaluate the accuracy of the presented model in the optimal condition.

EXPERIMENTAL SECTION

Experimental set-up

The designed experimental set-up to study the flow and convective heat transfer under constant wall temperature boundary condition in the tube is schematically shown in Fig. 1. The experimental set-up consisted of the test section, measurement equipment of temperature, pressure and flow rate, flow controlling system, and heating and cooling unite. A 6.75 liter reservoir tank equipped with a drain valve is used to store the working fluid. The working fluid has been forced through the loop with aid of a centrifugal pump (PKm60, Pedrollo), and its flow rate has been controlled by a ball valve. The length of entry section is 1m to guarantee the fully developed flow at the entrance of the test sections. The flow rate has been calculated by determining the time required to full a certain volume. The test section consisted of a copper tube with 1m length, 15 mm inner diameter and 1 mm thickness. The working fluid flowing inside the inner tube is heated through saturated steam inside annular section. This creates constant wall temperature boundary condition along the tested tubes. The outer tube has been well insulated by fiberglass in order to prevent heat loss. Two T-type thermocouples have been located at the inlet and outlet of the test section to measure the temperature of working fluid. Seven K-type thermocouples have been mounted on the copper tube wall to measure the wall temperature. The pressure drop is measured by using two very sensitive pressure transmitters (PSCH00.5BCIA, Sensys).

Nanofluid preparation

To prepare the nanofluids, a two-steps method has been applied. At first, the Al_2O_3 nanoparticles with the mean diameter of 40 nm has been carefully weighted, and next, they have been meticulously added to a volume of distilled water little by little. The material has been mixed completely for 45 min, and then the suspension has been located in an ultrasonic vibration apparatus (Hielschercompany, Germany) for 3 h in order to break down the bonds among particles. The desired weight concentrations were 0, 0.15 and 0.3 wt.%. With applying

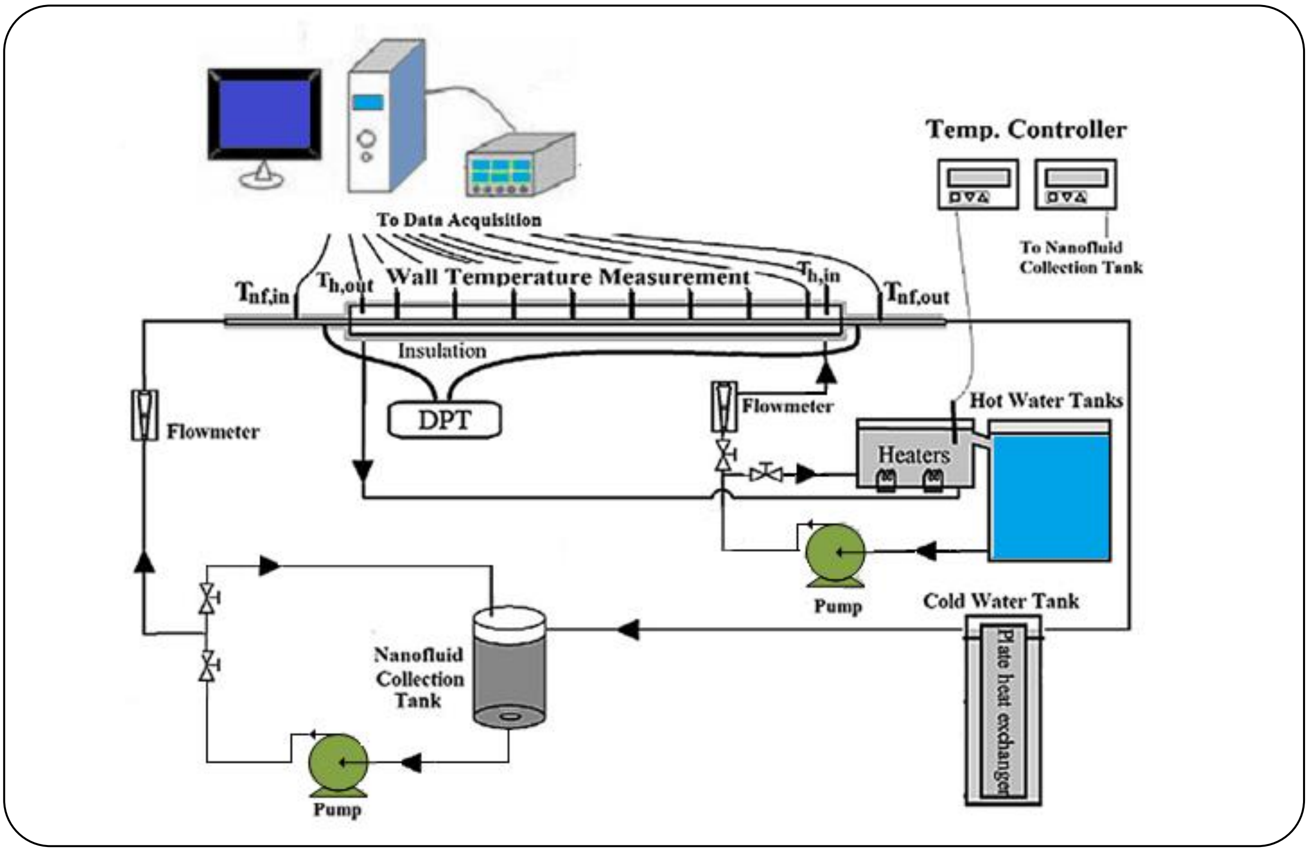

Fig. 1: Schematic of the experimental loop.

the stirrer and ultrasonic vibrator in this process results in more stable and uniform nanofluid. The prepared nanofluids have been stable for 72 h without any sedimentation.

Data reduction

The nanofluid flowing through the test sections absorbed the heat by steam condensation on the wall of channel. The absorbed heat by the nanofluid can be calculated as

$$Q = mC_p\left(T_{out} - T_{in}\right) \tag{1}$$

The average heat transfer coefficient is defined according to the following equation:

$$h = Q/A_t\left(T_w - T_f\right)_{LMTD} \tag{2}$$

where $(T_w - T_f)_{LMTD}$ is the logarithmic mean temperature difference and calculated as,

$$\left(T_w - T_f\right)_{LMTD} = \tag{3}$$

$$\left[\left(T_w - T_{in}\right) - \left(T_w - T_{out}\right)\right] / \log\left[\left(T_w - T_{in}\right)/\left(T_w - T_{out}\right)\right]$$

T_w is the average of seven measured temperatures on the wall of the channel at different positions. Also, the Nusselt number is defined according to the following equation:

$$Nu = hD_h/k \tag{4}$$

Where

$$D_h = 4A_cL/A_t \tag{5}$$

A_c is the minimum free flow area, L is the flow length, and A_t is the total heat transfer area.

Reynolds number can be calculated based on mass velocity (G) as follows,

$$Re = GD_h/\mu \tag{6}$$

Design Of Experiment (DOE)

The software Design Expert 8.0.4 has been used for experimental design. A 3-level factorial design has been used to evaluate the main effects and interaction (including volume fraction and Re number of nanofluid)

Table 2: Factors and levels for general factorial design.

Factor	Level		
	High (+1)	Centre (0)	Low (-1)
Reynolds (A)	8500	6500	4500
Solid volume fraction (B)	0.3	0.15	0

Table 3: Design layout and experimental results of 3-level factorial designs.

Std.	Run	Factorial input variable		Nu
		A	B	
1	5	-1	-1	38.1
2	6	0	-1	53.05
3	12	1	-1	70.5
4	4	-1	0	48.2
5	2	0	0	65.48
6	10	1	0	83.7
7	3	-1	1	51.2
8	9	0	1	69.8
9	7	1	1	87.8
10	8	0	0	65.8
11	1	0	0	65.2
12	11	0	0	66.1

on Nu number of Al_2O_3/water nanofluid. In this study, Reynolds number (range 4500-8500) and nanoparticle volume fraction (0-0.3) are variable input parameters, each of which includes three levels: −1 (low), 0 (central point) and 1 (high), with actual and coded values given in Table 2.

Table 3 shows the design layout and experimental results of Miscellaneous design (3-level factorial designs). To measure the process stability and inherent variability, three replicates have been added at the center point.

RESULTS AND DISCUSSION

Validation of the experimental system

In order to investigate the accuracy and reliability of the experiments, experiments have been performed for pure distilled water. Fig. 2 shows the experimental results of the average Nusselt number for the water compared with correlations reported in [21,22]. As can be seen, there is a good agreement between experimental data and theory for distilled water.

Residual analysis and model checking

The assumption of normality, constant error and completely randomized design have been checked by testing the residuals [23, 24]. Fig. 3 presents the normal probability percentage versus the internal studentized residuals for Nusselt numbers, confirming whether the statistical assumptions suit the analytical data or not. As it is seen in the figure, the studentized residuals nearly follow a normal distribution, because the points are creating an almost straight line.

The studentized residuals normal plot has been plotted versus run numbers to investigate the independence of the errors and the constant variance assumption. Fig. 4 illustrates the diagnostics plots of internally studentized residual versus the run number. As can be seen in the figure, there is no violation of the independence or constant variance assumption for all runs. Consequently, the model and assumptions are satisfied.

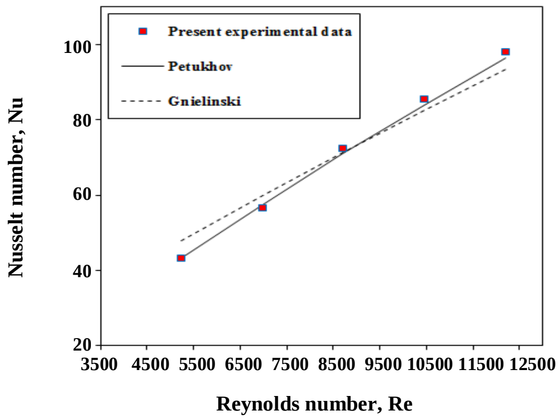

Fig. 2: Comparison between theoretical and experimental data for the Nusselt number of water.

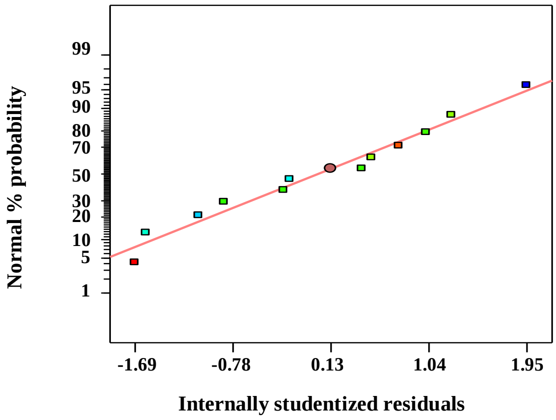

Fig. 3: Normal probability plot of internally stundentized residual for Nusselt number.

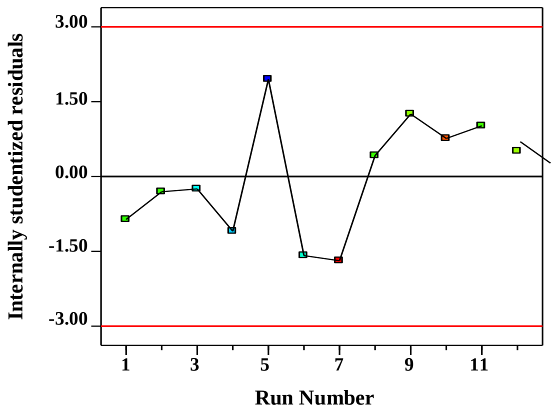

Fig. 4: Studentized residuals normal plot versos run number.

Analysis of variance (ANOVA)

In this study, by taking advantage of the Design-Expert software, the significance of the model has been carefully evaluated applying the analysis of variance. The ANOVA test results have been shown in Table 4. At first, the coefficient of determination (R^2) has been utilized to evaluate more accuracy of the model. F-value (Fisher variation ratio) and probability value (Prob > F) have been applied to investigate the significance of the model terms [9, 25]. From Table 4, the F-value of 197.22 and the "Prob > F" value of < 0.0001 show that the model is significant for the Nusselt number. Values of "Prob > F" less than 0.05 demonstrate the significant model's terms. Therefore, the effective terms of the model are Reynolds number (A), first and second order of effects of volume fraction (B, B^2), the interaction of Reynolds number and volume fraction (AB). In order to evaluate the fitness of the model, coefficient of determination (R^2), adjusted R^2 and predicted R^2 has been used. When R^2 is equal to 1, it indicates that 100% of the variability in the response could be explained by the model, so the predicted values are a well fit of experimental data [26]. In this model, R-squared (R^2) and adjusted R-squared (R^2-adj) are 0.9993 and 0.9986, respectively. Thus, the experimental data are well-fitted with the model. The value of R^2 emphasizes that only 0.07% of the total runs has not been explained by the model. "Adeq Precision (the signal to noise ratio) is desirable when it is greater than 4. The high accuracy (135.7) of this model indicates an adequate signal since it is larger than the boundary value of 4.

PROPOSED MODEL

A second order polynomial model has been obtained in terms of code that predicts the Nusselt number as a response, which is shown in equation 7.

$$Nu = 65.62 + 17.42A + 8.39B + 1.04AB + 0.37A^2 - 4.12B^2 - 0.79A^2B \quad (7)$$

Fig. 5 shows the predicted values versus the actual value of Nu number. As it is shown in this figure, the predicted Nu data is in good agreement with experimental data. The maximum error is around %0.3. According to equation No.7, by increasing factors A and B, the Nusselt number has been increased. And also, interaction effect of these two factors, have positive effects on the response variable.

Table 4: Analysis of variance (ANOVA).

Source	Sum of squares	df	Mean square	F-Value	p-value prob>F	
Model	2245.09	5	449	1616	<0.0001	Significant
A-A	1821.50	1	1821	6557	<0.0001	
B-B	371.04	1	371	1335.7	<0.0001	
AB	4.35	1	4.35	15.65	0.0075	
A^2	0.36	1	0.36	1.3	0.2971	
B^2	45.18	1	45.18	162.6	<0.0001	
Residual	1.67	6	0.28			
Lack of Fit	1.22	1	0.41	2.74	0.2145	not significant
Pure Error	0.45	3	0.15			
Cor Total	2246.76	11				
Std. Dev.	0.53	R^2	0.9993			
Mean	63.75	Adjust R^2-	0.9986			
C.V. %	0.83	Predict R^2	0.9941			
PRESS	13.27	Adequate Precision	135.7			

Table 5: The optimal condition for the Nusselt number.

Response	A (Re)	B (nanoparticle volume fraction)	experimental value	Predicted value
Nu	1	0.94	87.04	87.83

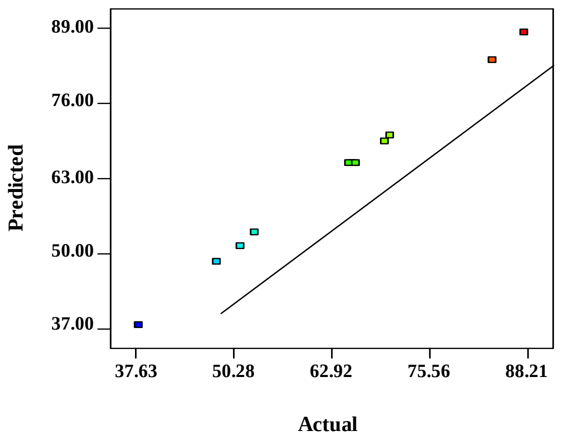

Fig. 5: Correlation between experimental and predicted values of Nu number.

It's reported that increasing Re and the nanoparticle percent in the base fluid cause increasing Nusselt number. Similarly, it's reported that by increasing Re number and the nanoparticle percent in the base fluid, the Nusselt number has been increased [10].

Optimization of the operational condition

Finally, by using the software Design Expert 8.0.4, the optimum experimental results have been calculated based on RSM strategy, and have been shown in Table 5. The optimum condition is the Reynolds number of 8500 and nanoparticle volume fraction of 0.282, (i.e. A: +1 and B: +0.94), under the optimal condition the Nu number is equal to 87.83 (Table 5), which is close to the actual value. Therefore, the optimal condition achieved with the model is a well-trusted outcome.

The Al_2O_3/water nanofluids at two different volumetric concentrations (i.e. 1.5% and 3%) have been examined in the present experimental work. The Reynolds number varies between about 3000 and 8500. The Nusselt numbers of nanofluids with respect to Reynolds number for two volume fractions are shown in Fig. 6. It is observed that the Nusselt numbers of all nanofluids are significantly higher than the base fluid. Therefore, Nusselt numbers of the nanofluid increase by increasing the Reynolds number and nanoparticle concentration. *Yetilmezsoy et al.* [27] reported that

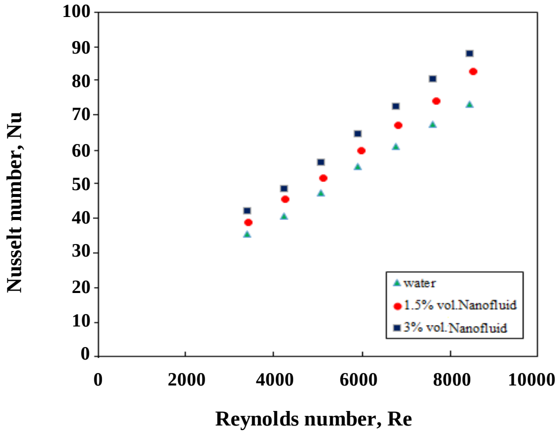

Fig. 6: The Nusselt number for Al_2O_3–water nanofluids versus Reynolds number at various volume concentrations.

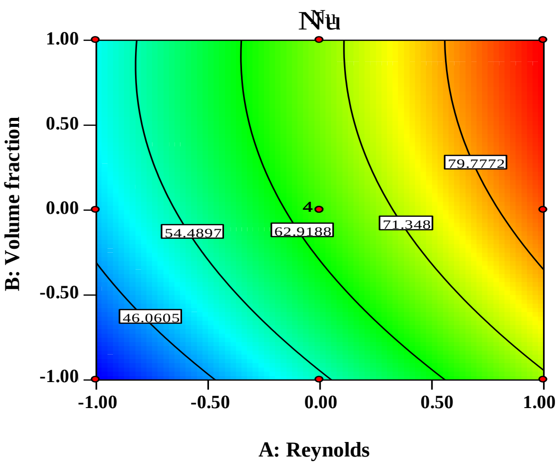

Fig. 7: Interaction effect of Reynolds and volume fraction of nanoparticles on Nusselt number contour plot.

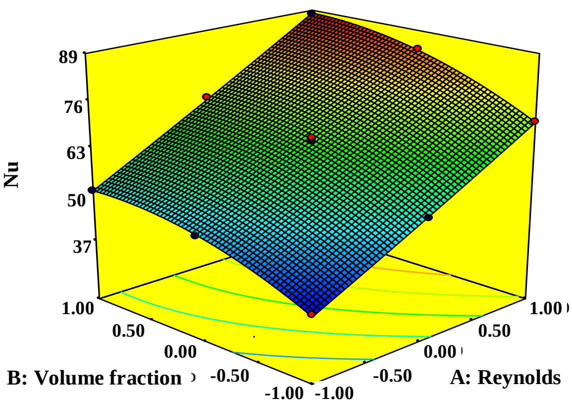

Fig. 8: Interaction effect of Reynolds and volume fraction of nanoparticles on the Nusselt number: 3-D surface.

the main and interactive effects of the two factors on the response could be investigated using the three dimensional (3D) response surface plots as a function of two factors, where the remaining factors are kept at a constant level. Figs. 7 and 8 show 3D and contour plots that illustrate the interactive influence of Reynolds number and volume fraction on Nu number. It can be observed that increasing the Re number and volume fraction, enhances Nu number. These figures clearly indicate that at any fixed Reynolds number, the Nusselt number of Al_2O_3/water nanofluid increases by increasing volume fraction and then it remains almost constant. The nonlinear nature of the 3D response surfaces and the respective contour plots can indicate the importance of the interaction effect of the two factors on the response. Also, the results indicated that when the Reynolds number is equal to 8500, the ascending trend of Nusselt number with volume fraction is more prominent.

CONCLUSIONS

Prediction of the effects of the main parameters on the Nusselt number is essential to investigate heat transfer. In this study, the experimental design was performed in order to evaluate the effect of the velocity and nanoparticle volume fraction on heat transfer of Al_2O_3/water nanofluids. A 3-level factorial design was used to evaluate the main effects and interaction (including volume fraction and velocity of nanofluid) on Nu number of Al_2O_3/water nanofluid. The optimum conditions of experimental results were predicted based on RSM method. In this condition, Reynolds number is 8500 and volume fraction is 0.282. An experiment in the optimal condition was performed to demonstrate the accuracy of the model. The results indicated that the model well predicts the Nusselt number in the optimum conditions. Finally, new correlation based on main effects and interactions with high accuracy was proposed to predict the Nusselt number.

Acknowledgments

This research was financially supported by Arak University. Authors of this work appreciate Arak University for their financial support.

Received : Jul. 8, 2017 ; Accepted : Jan. 10, 2018

REFERENCES

[1] Bergles A.E., Webb R.L., A Guide to the Literature on Convective Heat Transfer Augmentation, *Adv Enhanced Heat Transfer.*, **43**: 81-89 (1985).

[2] Mohebbi K., Rafee R., Talebi F., Effects of Rib Shapes on Heat Transfer Characteristics of Turbulent Flow of Al_2O_3-Water Nanofluid inside Ribbed Tubes, *Iran. J. Chem. Chem. Eng. (IJCCE),* **34**(3): 61-77 (2015).

[3] Reay D., Heat Transfer Enhancement-a Review of Techniques and Their Possible Impact on Energy Efficiency in the UK, *Heat Recovery Systems and CHP.*, **11**: 1-40 (1991).

[4] Yousefi N., Pazouki M., Alikhani Hesari F., Alizadeh M., Statistical Evaluation of the Pertinent Parameters in Bio-synthesis of Ag/MWf-CNT Composites Using Plackett-Burman Design and Response Surface Methodology, *Iran. J. Chem. Chem. Eng. (IJCCE),* **35**(2): 51-62 (2016).

[5] Khoshvaght-Aliabadi M., Hormozi F., Zamzamian A., Effects of Geometrical Parameters on Performance of Plate-Fin Heat Exchanger: Vortex-Generator as Core Surface and Nanofluid as Working Media, *Applied Thermal Engineering.*, **72**: 565-579 (2014).

[6]] Darzi A.R., Farhadi M., Sedighi K., Aallahyari S., Delavar M.A., Turbulent Heat Transfer of Al_2O_3–Water Nanofluid Inside Helically Corrugated Tubes: Numerical Study, *International Communications in Heat and Mass Transfer.*, **41**: 68-75 (2013).

[7] Sundar LS., Sharma K.,Turbulent Heat Transfer and Friction Factor of Al_2O_3 Nanofluid in Circular Tube with Twisted Tape Inserts, *International Journal of Heat and Mass Transfer*., **53**:1406-1416 (2010).

[8] Khoshvaght-Aliabadi M., Hormozi F., Zamzamian A., Experimental Study of Cu–Water Nanofluid Forced Convective Flow Inside a Louvered Channel, *International Journal of Heat and Mass Transfer.*, **51**: 423-432 (2015).

[9] Chol S., Enhancing Thermal Conductivity of Fluids with Nanoparticles, *ASME-Publications-Fed.*, **231**: 99-106(1995).

[10] Davarnejad R., Barati S., Kooshki M., CFD Simulation of the Effect of Particle Size on the Nanofluids Convective Heat Transfer in the Developed Region in a Circular Tube, *Springer Plus.*, **2**: (1)192 (2013).

[11] Leong KY., Che Ibrahim I., Amer NH., Risby M., Thermal Conductivity of Carbon Nanotube Based Nanofluids as Heat Transfer Fluids, *Applied Mechanics and Materials: Trans Tech Publ*; 29-33 (2016).

[12] Prasad P.D., Gupta A., Sreeramulu M., Sundar LS., Singh M., Sousa AC., Experimental Study of Heat Transfer and Friction Factor of Al_2O_3 Nanofluid in U-Tube Heat Exchanger with Helical Tape Inserts, *Experimental Thermal and Fluid Science*., **62**: 141-50 (2015).

[13] Wen D., Ding Y., Experimental Investigation into Convective Heat Transfer of Nanofluids at the Entrance Region under Laminar Flow Conditions, *International Journal of Heat and Mass Transfer.*, **47**: 5181-5188 (2004).

[14] Heris S.Z., Etemad S.G., Esfahany M.N., Experimental Investigation of Oxide Nanofluids Laminar Flow Convective Heat Transfer, *International Communications in Heat and Mass Transfer*., **33**: 529-535 (2006).

[15] Bianco V., Manca O., Nardini S., Numerical Investigation on Nanofluids Turbulent Convection Heat Transfer Inside a Circular Tube, *International Journal of Thermal Sciences.*, **50**: 341-349 (2011).

[16] Behzadmehr A., Saffar-Avval M., Galanis N., Prediction of Turbulent Forced Convection of a Nanofluid in a Tube with Uniform Heat Flux Using a Two Phase Approach, *International Journal of Heat and Fluid Flow.*, **28**: 211-219 (2007).

[17] Hemmat Esfe M., Saedodin S., Mahmoodi M., Experimental Studies on the Convective Heat Transfer Performance and Thermophysical Properties of MgO–Water Nanofluid under Turbulent Flow, *Experimental Thermal and Fluid Science*., **52**: 68-78 (2014).

[18] Hojjat M., Etemad S.G., Bagheri R., Thibault J., Convective Heat Transfer of Non-Newtonian Nanofluids Through a Uniformly Heated Circular Tube, *International Journal of Thermal Sciences*., **50**: 525-531(2011).

[19] Suresh S., Venkitaraj KP., Selvakumar P., Chandrasekar M., Effect of Al_2O_3–Cu/Water Hybrid Nanofluid in Heat Transfer, *Experimental Thermal and Fluid Science*., **38**: 54-60(2012).

[20] Duangthongsuk W., Wongwises S., Heat Transfer Enhancement and Pressure Drop Characteristics of TiO_2–Water Nanofluid in a Double-Tube Counter Flow Heat Exchanger, *International Journal of Heat and Mass Transfer.*, **52**: 2059-2067(2009).

[21] Gnielinski V., New Equations for Heat and Mass-Transfer in Turbulent Pipe and Channel Flow, *International Chemical Engineering*, **16**: 359-368 (1976).

[22] Petukhov B., Heat Transfer and Friction in Turbulent Pipe Flow with Variable Physical Properties, *Advances in Heat Transfer.*, **6**: 565- (1970).

[23] Rahmanian B., Pakizeh M., Mansoori SAA., Abedini R., Application of Experimental Design Approach and Artificial Neural Network (ANN) for the Determination of Potential Micellar-Enhanced Ultrafiltration Process, *Journal of Hazardous materials.*, **187**: 67-74 (2011).

[24] Abdollahi Y., Zakaria A., Aziz RaS., Tamili S., Matori KA., Shahrani N., et al. Optimizing Bi_2O_3 and TiO_2 to Achieve the Maximum Non-Linear Electrical Property of ZnO Low Voltage Varistor, *Chemistry Central Journal.*, **7**: 137- (2013).

[25] Kumar R., Leech D., A Glucose Anode for Enzymatic Fuel Cells Optimized for Current Production under Physiological Conditions Using a Design of Experiment Approach, *Bioelectrochemistry.*, **106**: 41-46 (2015).

[26] Rostamian H., Lotfollahi MN., New Functionality for Energy Parameter of Redlich-Kwong Equation of State for Density Calculation of Pure Carbon Dioxide and Ethane in Liquid, Vapor and Supercritical Phases, *Periodica Polytechnica Chemical Engineering.*, **60**: 93-97(2016).

[27] Yetilmezsoy K., Demirel S., Vanderbei RJ., Response Surface Modeling of Pb (II) Removal from Aqueous Solution by Pistacia Vera L.: Box–Behnken Experimental Design., *Journal of Hazardous Materials.*, **171**: 551-562 (2009).